A Geometric Interpretation of the Gouy Phase for Higher Order Hermite-Gaussian Modes

Nicolas J. Deshler

OPTI 600G
Spring 2022

Contents

Abstract

The Gouy phase shift is the phenomenon by which focused optical beams accrue a π phase shift relative to a plane wave propagating in the same direction with the same frequency. This work attempts to extend Boyd's [1] geometrical interpretation that the Gouy phase shift arises from the optical path difference between the beam waist trajectory and a ray trajectory when evaluated in the far field. In particular we explore whether this argument successfully extends to higher-order Hermite-Gauss modes through a numerical study.

1 Introduction

As a coherent Gaussian beam passes through a focus, the phase of the beam along the optical axis diverges from the phase of a plane wave propagating in the same direction with the same frequency. This phenomenon, known as the Gouy phase anomaly, was first described by Leon Georges Gouy in 1890. Gouy's principal result was that this phase difference ranges from $-\pi/2$ to $\pi/2$ as the beam propagates from $-\infty$ through the focus and onward to $+\infty$ via the equation

$$\phi_G(z) = \arctan\left(\frac{z}{z_0}\right) \tag{1}$$

Gouy's phase equation defines the origin of the coordinate system to be coincident with the beam focus; the point at which the beam waist is a minimum.

Since his discovery, there have been several different derivations of the Gouy phase that lend insight towards its physical origin. One of the most profound derivations was presentd by Feng and Winful [3]. In their work, they derive the Gouy phase equation from the uncertainty principle between a beam's transverse spatial confinement and the associated broadening of its transverse momentum. This alters the expectation value of the beam's axial momentum, which translates to a phase shift. Their approach is general enough to derive the Gouy phase anomaly for higher-order Gaussian modes such as the Hermite-Gauss (HG) and Laguerre-Gauss (LG) modes,

$$\phi_G^{[N]} = (2N+1)\phi_G(z) \tag{2}$$

where N is a generalized mode order index. For instance, the HG_{nm} mode has $N = n + m$ [3] while the $LG_{p\ell}$ mode has $N = 2p + |\ell|$ [4]. The modal dependence of these phase shift has given rise to several interesting applications including an LG mode sorter [4].

While Feng and Winful's work explicitly derives equation 1 for any transverse beam profile, Boyd [1] offers an intuitive geometrical argument for the origin of the *total* phase shift $\Delta\phi_G = \pi$ evaluated in the far-field. However, Boyd does so for the Gaussian beam alone. Specifically, the Boyd interpretation evaluates the optical path difference (OPD) between the hyperbolic trajectory traced by the beam waist and the linear trajectory that coincides with the far-field asymptotic behavior of the hyperbola.

The purpose of this report is to determine whether the total Gouy phase shift $\Delta\phi_G^{[N]} = (2N+1)\pi$ for higher-order modes can be derived using the same optical path difference (OPD) argument that Boyd presents for the Gaussian beam. In general, the footprint of Gaussian modes increases with the mode order. Thus, it stands to reason that the OPL of the hyperbolic beam waist trajectory for higher-order modes should be different from the OPL of the hyperbolic beam waist trajectory for the Gaussian beam .

2 Derivation of Gouy Phase for a Gaussian Beam

Consider a monochromatic complex Gaussian beam with wavenumber $k = \frac{2\pi}{\lambda}$ that is rotationally symmetric about the optical axis. We can express the beam as a scalar field under the assumption that it is uniformly polarized in some direction perpendicular to the z-axis.

$$U(\rho, z) = F(z)e^{ik\rho^2/2q(z)} \tag{3}$$

Here the Gaussian beam is described in cylindrical coordinates, where $\rho = \sqrt{x^2 + y^2}$ is the radial distance from the z-axis. We have also introduced the Gaussian parameter $Q(z) = \frac{1}{q(z)} = \frac{1}{R(z)} + \frac{2i}{kw^2(z)}$. All variables with z-dependence are real quantities with physical meaning.

$$w(z) : \text{Beam Spot Size}$$
$$R(z) : \text{Wavefront Radius of Curvature}$$
$$F(z) : \text{On-Axis Field Amplitude}$$

Each can be defined explicitly in terms of z.

$$w^2(z) = w_0^2 \left(1 + \left(\frac{z}{z_0} \right)^2 \right) \tag{4}$$

$$1/R(z) = \frac{z_0^2}{z} \left(1 + \left(\frac{z}{z_0} \right)^2 \right) \tag{5}$$

where w_0 is the beam waist at the focus and $z_0 = \pi w_0^2 / \lambda$ is the Rayleigh range. It is well known that the Gaussian beam profile we have defined is a solution to the paraxial wave equation

$$\nabla_\perp^2 U + 2ik \frac{\partial}{\partial z} U = 0 \tag{6}$$

where the perpendicular Laplacian is $\nabla_\perp^2 = \frac{\partial^2}{\partial x^2} + \frac{\partial^2}{\partial x^2}$ in Cartesian coordinates. Note that equation 3 is separable in x and y.

$$U(\rho, z) = U(x, z) U(y, z)$$

where

$$U(x, z) = F(z) e^{-ikx^2 / 2q(z)}$$
$$U(y, z) = e^{-iky^2 / 2q(z)}$$

Due to the symmetry of the Gaussian beam about the optical axis, we will derive the Gouy phase from the x dimension alone. Rearranging the paraxial equation and dropping the partial derivatives with respect to y we have

$$\frac{\partial}{\partial z} U(x, z) = \frac{i}{2k} \frac{\partial^2}{\partial x^2} U(x, z)$$

Applying the derivatives on both sides to $U(x, z)$ we find,

$$\left[\frac{\dot{F}}{F} - \frac{ik}{2} \frac{x^2}{q^2} \dot{q} \right] U(x, z) = - \left[\frac{1}{2q} + \frac{ik}{2} \frac{x^2}{q^2} \right] U(x, z)$$

where the dot notation indicates differentiation with respect to z. Matching the terms for like-powers of x we distill two first order differential equations which are solvable.

$$\dot{q} = 1 \qquad\qquad \implies q(z) = z + q_0 \qquad\qquad (7)$$

$$\dot{F} = -\frac{F}{2q} \qquad\qquad \implies F(z) = F_0\sqrt{\frac{q_0}{q(z)}} \qquad\qquad (8)$$

Taking $F_0 = 1$, we are left with $F(z) = \sqrt{q_0/q(z)}$. Inserting the definition of $q(z)$ we find that

$$F(z) = \frac{1}{\sqrt{1 + iz/z_0}}$$

Expressing the complex number inside the square root in polar form we have $1 + iz/z_0 = \sqrt{1 + (z/z_0)^2}e^{i\phi(z)} = \frac{w(z)}{w_0}e^{i\phi(z)}$ where $\phi(z) = \arctan(z/z0)$. Finally,

$$F(z) = \sqrt{\frac{w_0}{w(z)}}e^{-i\phi(z)/2}$$

where $\phi(z) = \phi_G(z) = \arctan(z/z0)$. Note that performing the same procedure on $U(y, z)$ yields an identical phase term which when multiplied through eliminates the factor of $1/2$ in the expression for $F(z)$.

3 The Boyd Interpretation

Recall the equation for the beam waist from equation 5

$$w(z) = w_0\sqrt{1 + (z/z_0)^2}$$

which is the equation of a hyperbola. The Boyd interpretation of the Gouy phase stems from the observation that there exists an optical path difference between the linear asymptote of the beam waist hyperbola and the hyperbola itself. In the far-field limit where $z >> 1$ we see that the hyperbola can be approximated by a linear function

$$w(z) \approx \frac{w_0}{z_0}z = \theta_{ff}z$$

where we have introduced θ_{ff}, the far-field angle. Figure 1 provides a visualization of this asymptotic limit.

We can find the OPL of these trajectories by integration over finite bounds. Since the divergence of a Gaussian beam is symmetric over the focus, we choose to integrate over symmetric interval $[-z_1, +z_1]$ along the optical axis for convenience (see figure 2). The beam waist OPL along the path BCD from figure 2 is

$$L = 2z_0\int_0^{z_1/z_0}\sqrt{\frac{1 + (1 + \theta_{ff}^2)x^2}{1 + x^2}}$$
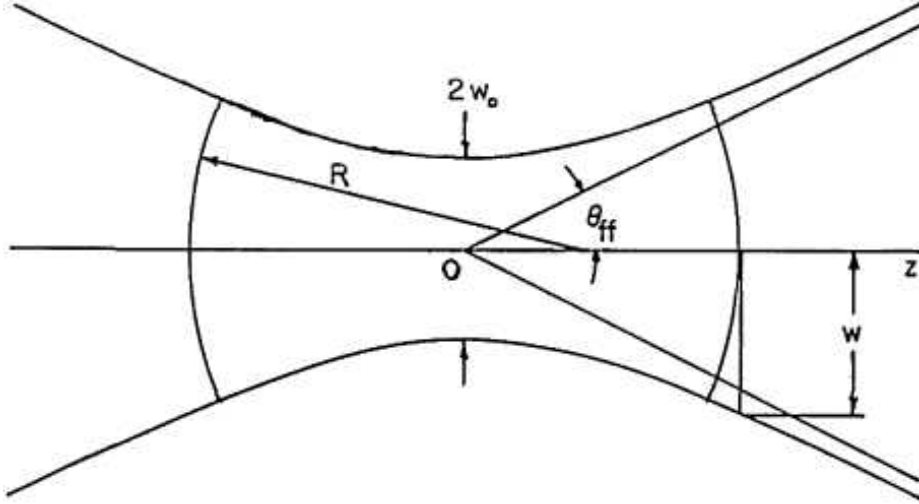
Figure 1: The equation for the beam waist forms a hyperbola as shown in the figure from reference [1]. The hyperbola asymptotically approaches a linear function in the limit of $z \to \infty, -\infty$.

This integral can be expressed in terms of elliptic integrals as

$$L = 2w_0\sqrt{1 + \theta_{ff}^{-2}}\left[\frac{1}{1 + \theta_{ff}^2}F(\phi, \kappa) - E(\phi, \kappa) + \frac{z_1}{z_0}\sqrt{\frac{(1 + \theta_{ff}^{-2})(w_0^2\theta_{ff}^{-2} + z_1^2)}{w_0^2\theta_{ff}^{-4} + z_1^2(1 + \theta_{ff}^{-2})}}\right]$$
(9)

where $F(\phi, \kappa)$ and $E(\phi, \kappa)$ are the elliptic integrals of the first and second kinds respectively and we have defined

$$\phi = \sin^{-1}\sqrt{z_1^2/[z_1^2 + w_0^2(\theta_{ff}^2 + \theta_{ff}^4)^{-1}]}$$

$$\kappa = \sqrt{\theta_{ff}/(1 + \theta_{ff}^2)}$$

The OPL of the ray along the straight-line path BE from figure 2 is given by the euclidean distance,

$$L' = 2\sqrt{z_1^2(1 + \theta_{ff}^2) + w_0^2}$$
(10)

The OPD between these two paths can be rewritten as phase through multiplication by $k = 2\pi/\lambda$. Boyd's primary conclusion is that the Gouy phase shift can be written as

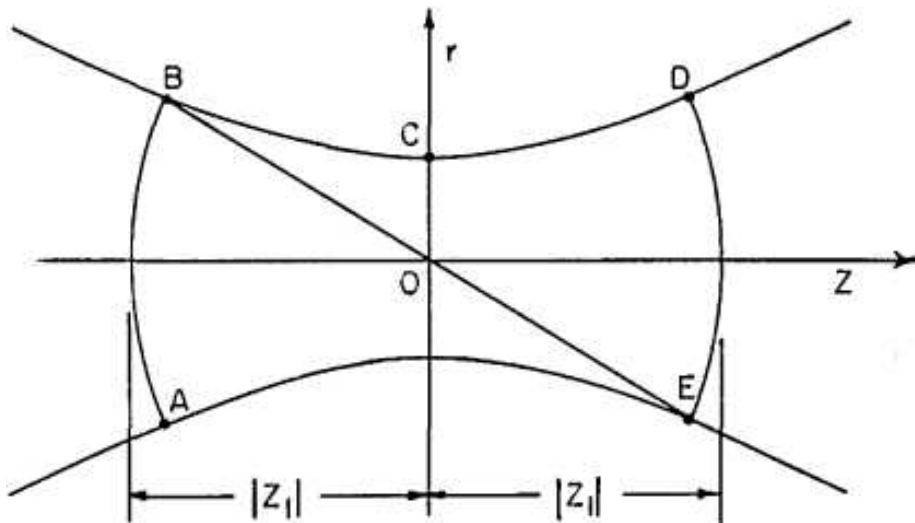$$\Delta\phi = \frac{2\pi}{\lambda}\lim_{z_1 \to \infty}(L' - L)$$
(11)

5

Figure 2: The curved path along BCD represents the trajectory of the beam waist while the straight line trajectory BE represents the trajectory of a the asymptotic ray. Boyd's interpretation posits that the OPD between these two trajectories evaluated in the limit as $z_1 \to \infty$ recovers the Gouy phase shift.

4   The Boyd Interpretation for Higher-Order HG Modes

The notion of beam waist for the Gaussian beam has an intuitive definition. Since the beam has a single peak, its waist is defined in relation to the FWHM. However, in the case of higher-order HG modes, such a definition is not so straightforward as these modes exhibit multiple peaks (see figure 3). Luxon and Parker have generalized the notion of beam waist to higher-order HG modes by considering the dominant support of the mode [5]. They define the waist for higher-order modes to be the distance from the center of the spot to the center of the outer-most peak. This definition allows us to ascribe a spot-size to any symmetric HG mode (i.e. $n = m$). Specifically, they find that the effective beam waist for a higher-order symmetric modes ($N = 2, 4, 6, \ldots$) takes the form

$$w_0^{[N]} = k_N w_0 \sqrt{2N + 1} \tag{12}$$

where k_N is a correction factor for each mode defined as $k_N = 1 + 0.73 N^{-0.78}$. Moreover, they find the effective Rayleigh Range to be

$$z_0^{[N]} = \frac{\pi}{\lambda} \left[\frac{w_0^{[N]}}{2N + 1} \right]^2 = k_N^2 z_0 (2N + 1)^{-1} \tag{13}$$

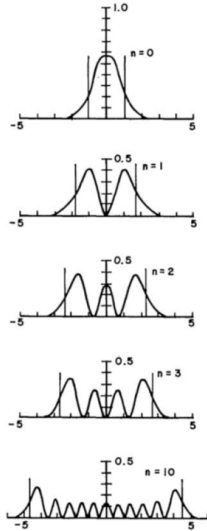With these parameters in hand, we can define the hyperbolic beam waist

6

Figure 3: A visualization of the beam waist definition in equation 12 for higher order HG modes. This figure, from reference [2], omits the correction factor K_N proposed by Luxon and Parker. Note that the footprint (beam waist) grows with the order number. This is what intuitively accounts for larger Gouy phase shifts at higher-orders.

trajectory for a higher-order mode as

$$w^{[N]}(z) = w_0^{[N]} \sqrt{1 + \left(z/z_0^{[N]}\right)^2} \tag{14}$$

and the far-field angle

$$\theta_{ff}^{[N]} = \frac{w_0^{[N]}}{z_0^{[N]}} = \left(\frac{w_0}{z_0}\right) \frac{(2N+1)^{3/2}}{k_N} \tag{15}$$

Equations 9, 10, and 11 were derived for a beam with waist w_0, rayleigh range z_0, far-field angle θ_{ff} and integration limit z_1. Thus we can simply exchange these parameters with their superscripted counterparts to find the OPD's for higher-order HG modes. This allows us to invoke the Boyd interpretation for higher-order HG modes and evaluate whether we can recover the same Gouy phase shift predicted by the Feng and Winful theory.

Figure 4 shows the hyperbolic trajectories for higher-order HG modes. Each of these has an associated asymptotic ray trajectory with slope $\theta_{ff}^{[N]}$. Figure 5 shows the Gouy phase shift predicted by the Boyd interpretation converging to the theoretical value for a select number of HG modes. This suggests that the Boyd interpretation is indeed valid for higher order HG modes. One possible extension to the work presented herein is assessing if the Boyd interpretation applies successfully to higher order LG modes. Since the LG modes have a

characteristic support that is rotationally invariant about the optical axis, we would not need to limit our discussion to symmetric modes as we did in the HG case. In other words, there would be no constraints on the viable LG indices (p, ℓ).
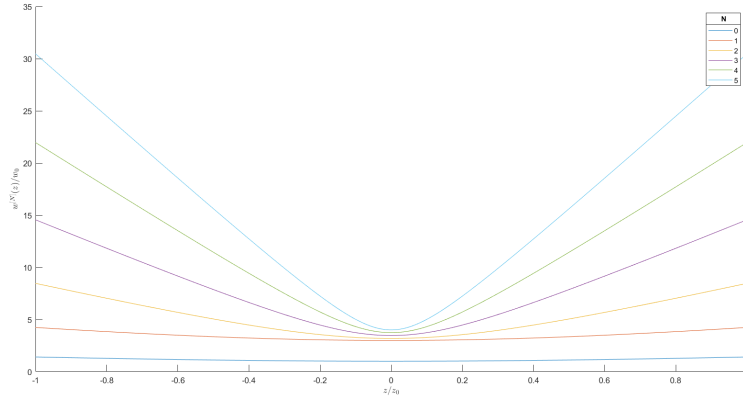

Figure 4: Beam waist hyperbolic trajectories for symmetric HG modes of different order. In general the beam waist hyperbolas exhibit sharper curvature and larger far-field divergence angles $\theta_{ff}^{[N]}$ for higher mode orders.
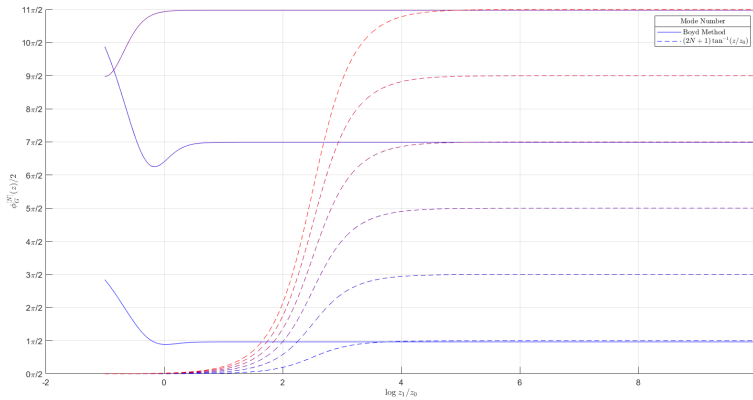

Figure 5: Convergence of Guoy Phase Shifts for HG modes of different order in the far field using the Boyd interpretation. We see that the Boyd interpretation converges to the proper Gouy phase shift when the OPD is evaluated over an interval of $5\times$ the Rayleigh range on either side of the focus.

References

[1] Robert W. Boyd. "Intuitive explanation of the phase anomaly of focused light beams". In: *J. Opt. Soc. Am.* 70.7 (July 1980), pp. 877–880. DOI: 10.1364/JOSA.70.000877. URL: http://opg.optica.org/abstract.cfm?URI=josa-70-7-877.

[2] William H. Carter. "Spot size and divergence for Hermite Gaussian beams of any order". In: *Appl. Opt.* 19.7 (Apr. 1980), pp. 1027–1029. DOI: 10.1364/AO.19.001027. URL: http://opg.optica.org/ao/abstract.cfm?URI=ao-19-7-1027.

[3] Simin Feng and Herbert G. Winful. "Physical origin of the Gouy phase shift". In: *Opt. Lett.* 26.8 (Apr. 2001), pp. 485–487. DOI: 10.1364/OL.26.000485. URL: http://opg.optica.org/ol/abstract.cfm?URI=ol-26-8-485.

[4] Xuemei Gu et al. "Gouy Phase Radial Mode Sorter for Light: Concepts and Experiments". In: *Phys. Rev. Lett.* 120 (10 Mar. 2018), p. 103601. DOI: 10.1103/PhysRevLett.120.103601. URL: https://link.aps.org/doi/10.1103/PhysRevLett.120.103601.

[5] James T. Luxon, David E. Parker, and John Karkheck. "Waist location and Rayleigh range for higher-order mode laser beams". In: *Appl. Opt.* 23.13 (July 1984), pp. 2088–2090. DOI: 10.1364/AO.23.002088. URL: http://opg.optica.org/ao/abstract.cfm?URI=ao-23-13-2088.

```matlab
%%%%%%%%%%%%%%%%%%%%%%%%%%%%%%%%%%%%%%%%%%%%%%%%%%%%%%%%%%%%%%%%%%%%%%%%%%%%%
% OPTI 600G - Laser Beams and Resonators
% Final Report
% Spring 2022
% Nico Deshler
%%%%%%%%%%%%%%%%%%%%%%%%%%%%%%%%%%%%%%%%%%%%%%%%%%%%%%%%%%%%%%%%%%%%%%%%%%%%%
%
% Description:
% The objective of my report is to explore the Gouy phase introduced for
% higher-order Gaussian modes. The following MATLAB code generates
% visualizations of the Gouy phase under the Boyd interpretation
% for Hermite-Gaussian transverse modes.
% These visualizations can be found in the paper.
%
%%%%%%%%%%%%%%%%%%%%%%%%%%%%%%%%%%%%%%%%%%%%%%%%%%%%%%%%%%%%%%%%%%%%%%%%%%%%%

%% Preliminaries
nb = 1;                 % refractive index of LIH media [unitless]
lambda = 1e-3;          % wavelength [m]
k = 2*pi * nb/lambda;   % wavenumber [1/m]
w0 = lambda;            % beam waist [m]
z0 = pi*w0^2*nb/lambda; % Rayleigh range [m]

%% HERMITE-GAUSS GOUY PHASE
% Reference:
% Simin  Feng  and  Herbert  G.  Winful. (2001)
% "Physical  origin  of  the  Gouy  phaseshift".
% doi:10.1364/OL.26.000485.
% url:http://opg.optica.org/ol/abstract.cfm?URI=ol-26-8-485.2

phi_HG = @(m,n,z) -(m+n+1)*arctan(z/z0);

%% LAGUERRE-GAUSS GOUY PHASE
% Reference:
% Xuemei  Gu  et  al. (2018)
% "Gouy  Phase  Radial  Mode  Sorter  for  Light:  Concepts  and  Experiments".
% doi:10.1103/PhysRevLett.120.103601.
% url:https://link.aps.org/doi/10.1103/PhysRevLett.120.103601.3

phi_LG = @(p,l,z) (2*p + abs(l) + 1)*arctan(z/z0);

%% Boyd Picture - Gouy Phase = OPL between

% Calculate generalized beam waist for higher-order HG modes
% Reference:
% "Waist location and Rayleigh Range for higher-order mode laser beams"
% Luxon et. al (1994)
```

```matlab
% Applied Optics Vol 23, No. 13

% Handle functions are only valid for j>0
k_j = @(j) 1 + [zeros(j==0),ones(j~=0)*0.73*j^(-.78)];  % Correction factor for j'th ⤶
HG mode
w_j = @(j) k_j(j)*sqrt(2*j+1)*w0;                       % Beam Waist for j'th HG mode
z_j = @(j) k_j(j)^2/(2*j+1) * z0;                       % Rayleigh Range for j'th HG ⤶
mode

theta_j = @(j) w_j(j)/z_j(j);                          % Far-Field Boyd Angle for ⤶
j'th HG mode
wz = @(z,j) w_j(j) * sqrt(1+(z/z_j(j)).^2);            % Propagation equation for ⤶
j'th HG mode

% parameters for elliptic integrals
phi = @(zf,j) asin( zf.^2 ./ (zf.^2 + w_j(j)^2 * (theta_j(j)^2 +theta_j(j)^4)^(-1)));
kappa = @(j) sqrt( theta_j(j)^2 / (1 + theta_j(j)^2) );

% OPL of straightline asymptotic ray path
L = @(zf,j) 2* sqrt(zf.^2 * (1+ theta_j(j)^2) + w_j(j)^2);


% OPL of beam waist trajectory for HG mode j, with final z position equal to zf
%NOTE: ELLIPTIC INTEGRAL FUNCTIONS IN MATLAB ARE FUNCTIONS WITH ARGUMENTS
%PHI and M where M=KAPPA^2.
LL = @(zf,j) 2* w_j(j) * sqrt(1 + theta_j(j)^(-2)) * ...
    ( 1/(1 + theta_j(j)^2) * ellipticF(phi(zf,j), kappa(j)^2) - ellipticE(phi(zf,j), ⤶
kappa(j)^2)...
    + zf/z_j(j) .* sqrt( (1+theta_j(j)^(-2))*(w_j(j)^2*theta_j(j)^(-2)+ zf.^2) ./ ⤶
(w_j(j)^2 * theta_j(j)^(-4) +  zf.^2 * (1+theta_j(j)^(-2)))  )...
    );

% limiting case of OPD (evaluated in the far field)
delta_phi = @(j) -4/theta_j(j)^2  * sqrt(1+theta_j(j)^2) * (1/(1+theta_j(j)^2)* ⤶
ellipticF(pi/2,kappa(j)^2)-ellipticE(pi/2,kappa(j)^2));

% Guoy phase as a function of distance zf from beam waist for j'th HG mode
Gouy_phase_j = @(zf,j) 2*pi/lambda * (L(zf,j)-LL(zf,j));
hGouy_phase_j = @(zf,j) Gouy_phase_j(zf,j)/2;

% Highest Mode Order in Study
J = 5;

%% Make hyperbolic waist trajectory comparison figure
z = z0*linspace(-1,1,1000);

figure;

hold on
```

```matlab
for j = 0:J
    plot(z/z0,wz(z,j)/w0);
end
hold off

title('Beam Waist Trajectories for HG Modes')
xlabel('$z/z_0$','interpreter','latex')
ylabel('$w^{[N]}(z)/w_0$','interpreter','latex')

leg1 = legend(strsplit(num2str(0:J)));
title(leg1,'Mode Number')


%% Make Half Gouy Phase Shift Convergence Figure

% distance along optical axis that at which we evaluate net Gouy phase
log_zff = linspace(-1,10,1000);
zff = z0*10.^log_zff;
figure;
hold on
for j = 0:J
    c = (j/J)*[1;0;0] + (1-j/J)*[0;0;1];
    hGphase_Boyd = hGouy_phase_j(zff,j);
    Gphase_Theory = (2*j+1)*atan(zff);
    plot(log_zff,hGphase_Boyd,'','color',c)
    plot(log_zff,Gphase_Theory,'--','color',c);
end

title('Comparative Cumulative Phase - Boyd Method vs. Analytic Solution')
xlabel('$\log{z_1/z_0}$','interpreter','latex')
ylabel('$\phi_G^{[N]}(z) / 2$','interpreter','latex')
grid on

ylim([0,(2*J+1) * pi/2])
hpi_range = 0:(2*J+1);
yticks(pi/2*hpi_range);
C1 = strsplit(num2str(hpi_range));
C2 = cell(1,numel(hpi_range));
C2(:) = {'\pi/2'};
C = strcat(C1,C2);
yticklabels(C)
leg = legend({'Boyd Method','$(2N+1) \tan^{-1}(z/z_0)$'},'interpreter','latex');
title(leg,'Mode Number')


%% Testing Boyd Plots
kappa2 = @(theta) sqrt((theta.^2) ./ (1+ theta.^2));
delta_phi2 = @(theta) -4 ./ (theta.^2) .* sqrt(1+theta.^2) .* (1./(1+theta.^2) .* ↵
ellipticF(pi/2,kappa2(theta).^2)-ellipticE(pi/2,kappa2(theta).^2));
```

```matlab
figure;
theta = 10.^linspace(-5,1,1000);
plot(log((2*theta).^(-1)),delta_phi2(theta));
title('')
xlabel('$\log{2 \theta^{-1}}$','interpreter','latex')
ylabel('$\Delta \phi_G$','interpreter','latex')
```